

Influence of Parameter on The Chemical Activation of Mesoporous Carbon Material Derived from Cattail Leaves

Dolrudee Jaruwat¹, Apiluck Eiad-ua^{2,*}, Worapon Kiatkittipong³, Atthapon Srifa⁴, Sumittra Jarojrochkul⁵ and Suttichai Assabumrungrat¹

¹*Center of Excellence in Catalysis and Catalytic Reaction Engineering, Department of Chemical Engineering, Faculty of Engineering, Chulalongkorn University, Phayathai Rd., Phatumwan, Bangkok, 10330, Thailand*

²*College of Nanotechnology, King Mongkut's Institute of Technology Ladkrabang, Bangkok and 10520, Thailand, E-mail: apiluck.ei@kmitl.ac.th*

³*Department of Chemical Engineering, Faculty of Engineering and Industrial Technology, Silpakorn University, Nakhon Pathom 73000, Thailand*

⁴*Department of Chemical Engineering, Faculty of Engineering, Mahidol University, Nakhon Pathom 73170, Thailand*

⁵*National Metal and Materials Technology Center (MTEC), Pathum Thani and 12120, Thailand*

Abstract

The used of biodiesel in any diesel engines still have limitation due to the oxidative stability, cloud point, pour point, etc. Hydrogenation is one of the most efficient process, which require an effective metal catalyst impregnated on support materials with high specific surface area and large porosity. Carbon material such as mesoporous carbon has been recognized as an effective material that widely used in many applications including adsorbent, electrode and catalytic support. In this research, mesoporous carbon has been successfully synthesized from cattail leave via hydrothermal at 200°C for 12 h and substituted to chemical activation with various activating agent (i.e. H₂SO₄, H₃PO₄, NaOH and KOH) in N₂ atmospheric for 2 h at 500, 700 and 900°C, respectively. The optimum condition was 4M of KOH at 900°C for 2 h with specific surface area, average pore diameter and pore volume of 1323.58 m²/g, 2.78 nm and 0.672 cm³/g, respectively, which 3D network-like mesoporous structure. From this investigation, the synthesized mesoporous carbon will be an efficient material for catalytic support in biodiesel synthesis.

Keywords: Cattail leave, Mesoporous carbon, Chemical activation, Hydrothermal carbonization

1. Introduction

Nowadays, biodiesel is one of the renewable energy, which reduces the consumption of diesel fuel greatly. Although, the significant property is lubrication and complete combustion in diesel engines, oxidation stability also has a limited storage period.

Partial hydrogenation reactions can improve oxidation stability and cold flow properties appropriately because polyunsaturated fatty acid methyl esters convert to mono unsaturated fatty acid methyl esters over heterogeneous catalyst. The activity of the solid catalyst depends on the active site significantly. In addition, the supporting material are important to heterogeneous catalysis because it determines the distribution of the active phases. Hydrogenation reaction uses commonly inorganic support materials (ie. Al_2O_3 , SiO_2 , and MCM-41) (Alshaibani et al. 2017). The disadvantages of the supports are microporous with low surface area ($100\text{-}400\text{ m}^2\text{g}^{-1}$) resulting in metal agglomerate and block the pore. In addition, the support interacts weakly with metal particles. Mesoporous carbon is especially attractive for a variety of applications (ie. adsorbent, electrode and catalytic support) due to the high surface area ($500\text{-}2000\text{ m}^2\text{g}^{-1}$) and large pore size (2-50 nm). Activated carbon (AC) has high thermal stability due to the production process treated at high temperatures. In particular, using carbon as catalyst support will reduce the cost production, since the raw materials are agricultural. AC is complex the surface chemistry with an oxygenated functional group, which contains valence electrons that interact strongly with the reactant and metal particles (Olaf Deutschmann 2009). In this research, cattail leave (CL) is a source of carbon which is a weed that grows rapidly in canals. It also adds value to and reduces environmental pollution. Another reason, the main components contain high cellulose and lignin, which can create significant porosities by heating processes. Microwave is one of the methods of uniform heating, low operating time and saving energy. Large scale production is also difficult, including the soft template are simple to pore size control and complex synthesis. This study is focusing on the hydrothermal carbonization with chemical activation. The advantages of thermochemical are high surface area and yield. The chemical activation can generate many pores 4-50 times when compared to the non-chemical activation. This method has a temperature difference between the outside and inside of carbon, which provides a variety of pore sizes (Tang et al. 2018). The purpose of this research is to synthesize mesoporous carbon and control pore size with activating agent (i.e. H_2SO_4 , H_3PO_4 , NaOH and KOH).

2. Materials and Methods

2.1. Materials

Cattail leaves (CL) were collected from Ladkrabang in Thailand. Sulfuric acid (HS) 98%, Orthophosphoric acid (HP) 85% analytical grad, Sodium hydroxide anhydrous (NO) and Potassium hydroxide (KO) anhydrous pellets (Sigma-Aldrich, USA) acts as activating agents.

2.2. Methods

CL were dried to constant weight under room temperature, cut and crushed to powder. Next step, the CL powder were sieved into the size of 100 mesh. 30 g of CL powder and 60 ml of DI water were mixed and carried into the reactor. The reactor was heated to $200\text{ }^\circ\text{C}$ for 12 h under self-generated pressure, then cooled to room temperature and dried to remove moisture. 10 g of hydrochar (HC) were stirred with 100 ml of

activating agent (2, 4 and 6 M) at 80°C for 3 h. After stirring, The sample were filtered and dried in oven at 110°C for 24 h. All samples were placed in a horizontal tubular reactor followed by purging pure nitrogen gas at the 500°C, 700°C and 900°C for 2 h with heating rate 10 °C/min. Final, The sample were washed several times with deionized water and dried in the oven at 110°C for 24 h to obtained porous carbon.

2.3. Characterization

The morphology was verified by scanning electron microscope (EVO MA10). The magnification of the electron beam accelerated with an electric potential of 20 kV were 500x, 1000x and 2000x.

The porosity of activated carbon was determined by N₂ adsorption at 77 K. The surface area were estimated by Brunauer–Emmett–Teller (BET). The micropore volume (V_{micro}) was determined by BJH model. The mesopore volume (V_{meso}) was calculated as follows:

$$V_{\text{meso}} = V_{\text{total}} - V_{\text{micro}} \quad (1)$$

The proximate analysis of dry solid were analyzed by thermogravimetric analysis (SDT-Q600). The samples were heated from 30°C to 800°C under N₂ atmosphere before switching the air until 1000°C with a heating rate of 10 °C/min.

The ultimate analysis were analyzed by elemental analysis (CHNS628 series). The sample were burned to 950 °C under He and O₂ atmosphere quickly.

3. Result and Discussion

3.1. Effect of Activating Agent

Table 1 Effect of activation (activating agent, and temperature) on surface area of AC.

Sample	SSA (m ² g ⁻¹)	Pore size diameter (nm)	V_{total} (cm ³ g ⁻¹)	V_{micro} (cm ³ g ⁻¹)	V_{meso} (cm ³ g ⁻¹)
KO700-4	995	2.49	0.49	0.09	0.40
KO900-4	1323	2.78	0.78	0.06	0.72
NO700-4	975	2.57	0.63	0.21	0.42
NO900-4	1219	2.60	0.67	0.24	0.43
HS500-4	429	1.01	0.27	0.13	0.14
HS700-4	352	1.19	0.19	0.13	0.06
HP500-4	845	1.15	0.45	0.33	0.12
HP700-4	396	1.24	0.22	0.11	0.11

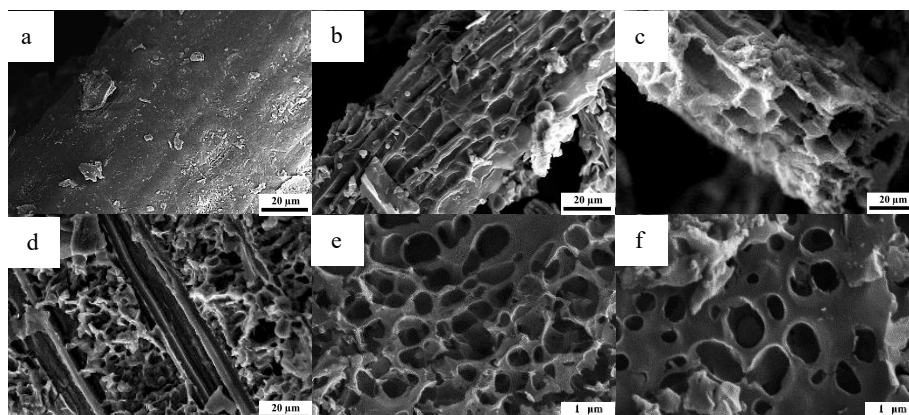
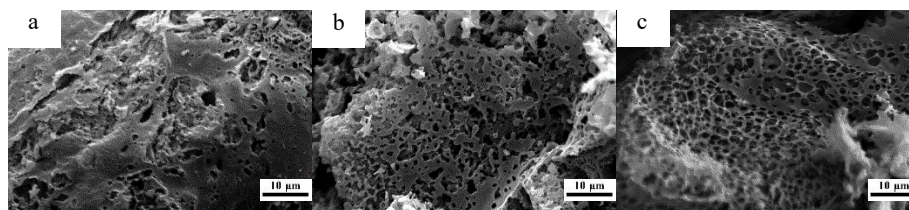


Fig. 2 SEM images of (a) CL (b) HC (c) HS500-4 (d) HP500-4 at 500x, (e) KO900-4 and (f) NO900-4 at 10000x magnification.

Table 1 indicate that acid activation generates all almost of the micropore, while base activation formed all almost of the mesopore (Karagöz et al. 2008). Base activation formed the high surface area and pore volume because the metal oxide decomposed to M_2CO_3 and M_2O . These products also reacted with steam and CO_2 lead to physical and chemical activation. KOH and NaOH have developed the surface area at 900 °C up to $1323.58 \text{ m}^2\text{g}^{-1}$ and $1219.61 \text{ m}^2\text{g}^{-1}$ respectively. KOH were the most effective in the development of surface areas followed by NaOH, H_3PO_4 and H_2SO_4 , respectively. The SEM image of AC are presented in Fig. 2(b). the hydrothermal process has provided the atrophy of the CL fibres because of the hydrolysis, dehydration and condensation reactions. Result in polymer chain of lignocellulose broke to short polymer as in Fig 2(b). AC has derived from acid and base activation. The base activation at 900°C generated external and internal pore as 3D network-like mesoporous structure. In the Fig. 2(e) KO900-4 has a uniform distribution of pores in comparison to NO900-4 due to kinetic energy of K^+ ions is higher than Na^+ ions at the same temperature. K^+ ions effectively inserted into the biomass (Namazi, Allen, and Jia 2016). The phosphoric acid created more external pore than sulfuric acid due to phosphoric acid is a weak acid ($K_a = 7.5 \times 10^{-3}$) and long reaction time.

3.2. Effect of Temperature



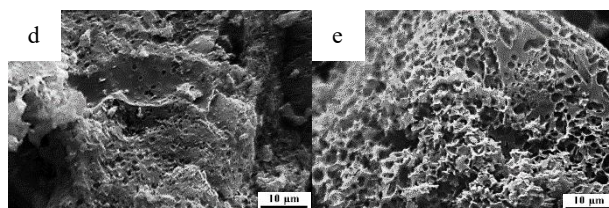


Fig. 3 SEM image of AC (a) KO500-4 (b) KO700-4 (c) KO900-4 (d) KO900-2 and (e) KO900-6 at 1000x magnification.

Table 1 shows that the KOH activation increased the surface area and pore volume at the high temperature because K_2CO_3 and K_2O decomposed to K^+ with high kinetic energy. The K^+ ion penetrated to generate the internal pores thoroughly, the pores gradually expanded when the temperature rised from 700 to 900°C as shown in Fig. 3(c). The pore evenly dispersed on the surface when increased the temperature reaction.

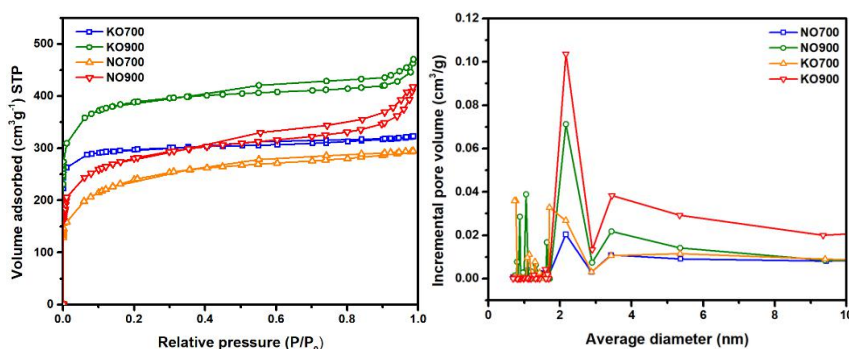


Fig. 4 (a) N_2 Adsorption-desorption isotherms and (b) Pore size distributions of AC.

Thermogravimetric analysis of base activation are presented in table 2. Moisture content and light mass volatile of all sample evaporated during 30–150°C due to dehydration reaction. High mass volatile decomposed during 200–500°C (CO , CO_2 , and some hydrocarbon, etc.). The hydrothermal process released the volatile matter by 15.59%wt. of weight loss. Hemicellulose composed of amorphous structure, which decomposed easily under temperatures 200–280°C. Cellulose consisted of a long polymer of glucose with well-ordered, which were very strong and decomposed during 280–500°C. Lignin decomposed slowly in a wide temperature range during 160–800 °C due to consisting of aromatic rings with different branches (Pazó et al. 2010).

In the Fig. 4(a) N_2 adsorption-desorption isotherm were calculated by Brunauer Emmett Teller method (BET) at 77 K. Chemical activation with base showed type I and IV isotherm, which indicated micro (< 2 nm) and mesopore (2–50 nm). Hysteresis loop represented as mesopore volume (V_{meso}) in a relatively high P/P_0 region.

Increasing the activation temperature enhanced the surface area and meso pore volume due to the loop area of the activation temperature 900°C were larger than 700 °C. In addition, N₂ adsorption enlarged rapidly at a relative pressure of less than 0.1, which revealed the micropore. In fig. 4(b) Pore size distribution were calculated by DFT method. Most of all were mesopore with narrow size in the range of 1.7-2.9 nm. In contrast, Acid activation created porous efficiently with dehydration, devolatilization and condensation reactions at 500 °C. The porosity shrinkage because the acid sited evaporated quickly at temperatures exceeding 500°C (Nahil and Williams 2012).

3.2. Effect of Concentration

The surface area and pore volume was reduced at low concentration because K⁺ ions were insufficient to form the internal pore. In Fig 4(d) shows that the external pore was irregular on the surface at 2 M. In addition, In Fig 4(e) shows that the surface area and pore volume diminished a little at 6 M due to the excessive ions oxidized inside the pores and provided the collapse of the pore.

Table 2 Ultimate and proximate analysis of AC with base activation.

Sample	Ultimate analysis (wt%)				Proximate analysis (wt%)			
	C	H	N	O*	FC%	VM%	M%	A%
CL	39.95	4.46	1.74	53.85	20.31	75.90	1.58	2.21
HC	45.45	4.40	1.83	48.32	33.28	62.31	1.63	2.78
KO500-4	58.86	4.69	1.69	34.76	72.89	19.97	1.01	6.13
KO700-4	69.19	4.18	1.31	25.32	78.64	13.67	1.43	6.26
KO900-4	86.35	4.67	1.64	7.34	81.18	10.41	1.59	6.82
KO900-2	77.61	4.26	1.49	16.64	79.84	13.98	1.29	4.89
KO900-6	81.63	4.22	1.28	12.87	82.98	7.64	1.85	7.53

In table 2. Hydrochar was released the volatile organic matter to gas product (H₂, CO, CO₂) and some light hydrocarbon (CH₄, C₂H₄, and C₂H₆), which reduced oxygen content at the 500°C. The high temperature increased the fixed carbon and carbon content due to the decomposition of biomass released tar and remained solid carbon (Muniandy et al. 2014; Somasundaram et al. 2013). Weight loss of volatile matter generated the porosity of carbon according to BET analysis. Ash remained after air combustion, which consisted of MgO, CaO, K₂O, and SO₃. Improving the concentration provided higher carbon content and ash residue, which indicated the product impurity.

5. Conclusions

This work demonstrates that mesoporous carbon derived from chemical activation with base at high temperatures. On the other hand, acid activation generated micropore efficiently at low temperatures. The activation temperature greatly affected the breakdown of lignocellulose, which created significantly surface area and pore volume. Although high concentrations also promoted porosity, it must consider the impurity residues after chemical activation. Moreover, other factors controlled the pore size of carbon such as during time, feedstock, gas flow rate and heating rate, etc.

6. Acknowledgment

The authors would like to acknowledge the funding given by The Thailand Graduate Institute of Science and Technology (TG-33-09-61-062M) for this project and the scholarship funding. The authors wish to thank the College of nanotechnology, King Mongkut's Institute of Technology Ladkrabang (KMITL), National Science and Technology Development Agency (NSTDA) and Center of Excellence in Catalysis and Catalytic Reaction Engineering, Department of Chemical Engineering, Faculty of Engineering, Chulalongkorn University for their support on instrumental analysis.

7. References

- Alshaibani, Abdulmajid, Zahira Yaakob, Ahmed Alsobaai, and Miskandar Sahri. 2017. 'Effect of chemically reduced palladium supported catalyst on sunflower oil hydrogenation conversion and selectivity', *Arabian Journal of Chemistry*, 10: S1188-S92.
- Karagöz, Selhan, Turgay Tay, Suat Uçar, and Murat Erdem. 2008. *Activated Carbons from Waste Biomass by Sulfuric Acid Activation and Their Use on Methylene Blue Adsorption*.
- Muniandy, Lingeswaran, Farook Adam, Abdul Rahman Mohamed, and Eng-Poh Ng. 2014. 'The synthesis and characterization of high purity mixed microporous/mesoporous activated carbon from rice husk using chemical activation with NaOH and KOH', *Microporous and Mesoporous Materials*, 197: 316-23.
- Nahil, Mohamad Anas, and Paul T. Williams. 2012. 'Pore characteristics of activated carbons from the phosphoric acid chemical activation of cotton stalks', *Biomass and Bioenergy*, 37: 142-49.
- Namazi, Azadeh, D. Allen, and Charles Jia. 2016. *Benefits of microwave heating method in production of activated carbon*.
- Olaf Deutschmann, Helmut Knozinger, Karl Kochloeflthomas Turek. 2009. 'Heterogeneous Catalysis and Solid Catalysts, 1. Fundamentals.' in, *Ullmann's Encyclopedia of Industrial Chemistry*.
- Pazó, Jose A., Enrique Granada, Angeles Saavedra, Pablo Eguía, and Joaquín Collazo. 2010. 'Biomass thermogravimetric analysis: uncertainty determination methodology and sampling maps generation', *International Journal of Molecular Sciences*, 11: 2701-14.
- Somasundaram, S., K. Sekar, V. K. Gupta, and S. Ganesan. 2013. 'Synthesis and characterization of mesoporous activated carbon from rice husk for adsorption of glycine from alcohol-aqueous mixture', *Journal of Molecular Liquids*, 177: 416-25.
- Tang, Zo-Ee, Steven Lim, Yean-Ling Pang, Hwai-Chyuan Ong, and Keat-Teong Lee. 2018. 'Synthesis of biomass as heterogeneous catalyst for application in biodiesel production: State of the art and fundamental review', *Renewable and Sustainable Energy Reviews*, 92: 235-53.